

## Electronic Supporting Information

### Formation of Liquid Marbles & Aggregates: Rolling and Electrostatic Formation Using Conductive Hexagonal Plates

*Benjamin T. Lobel<sup>1</sup>, Junya Fujiwara<sup>2</sup>, Syuji Fujii<sup>3,4</sup>, Casey A. Thomas<sup>1</sup>, Peter M. Ireland<sup>1</sup>, Erica J. Wanless<sup>1</sup>, Grant B. Webber<sup>1\*</sup>*

<sup>1</sup>Priority Research Centre for Advanced Particle Processing and Transport, University of Newcastle, Callaghan, NSW 2308, Australia.

<sup>2</sup>Division of Applied Chemistry, Graduate School of Engineering, Osaka Institute of Technology, 5-16-1 Omiya, Asahi-ku, Osaka 535-8585, Japan

<sup>3</sup>Department of Applied Chemistry, Faculty of Engineering, Osaka Institute of Technology, 5-16-1 Omiya, Asahi-ku, Osaka 535-8585, Japan

<sup>4</sup>Nanomaterials Microdevices Research Center, Osaka Institute of Technology, 5-16-1 Omiya, Asahi-ku, Osaka 535-8585, Japan

\*corresponding author: [grant.webber@newcastle.edu.au](mailto:grant.webber@newcastle.edu.au)

# Micrographs of PET plates

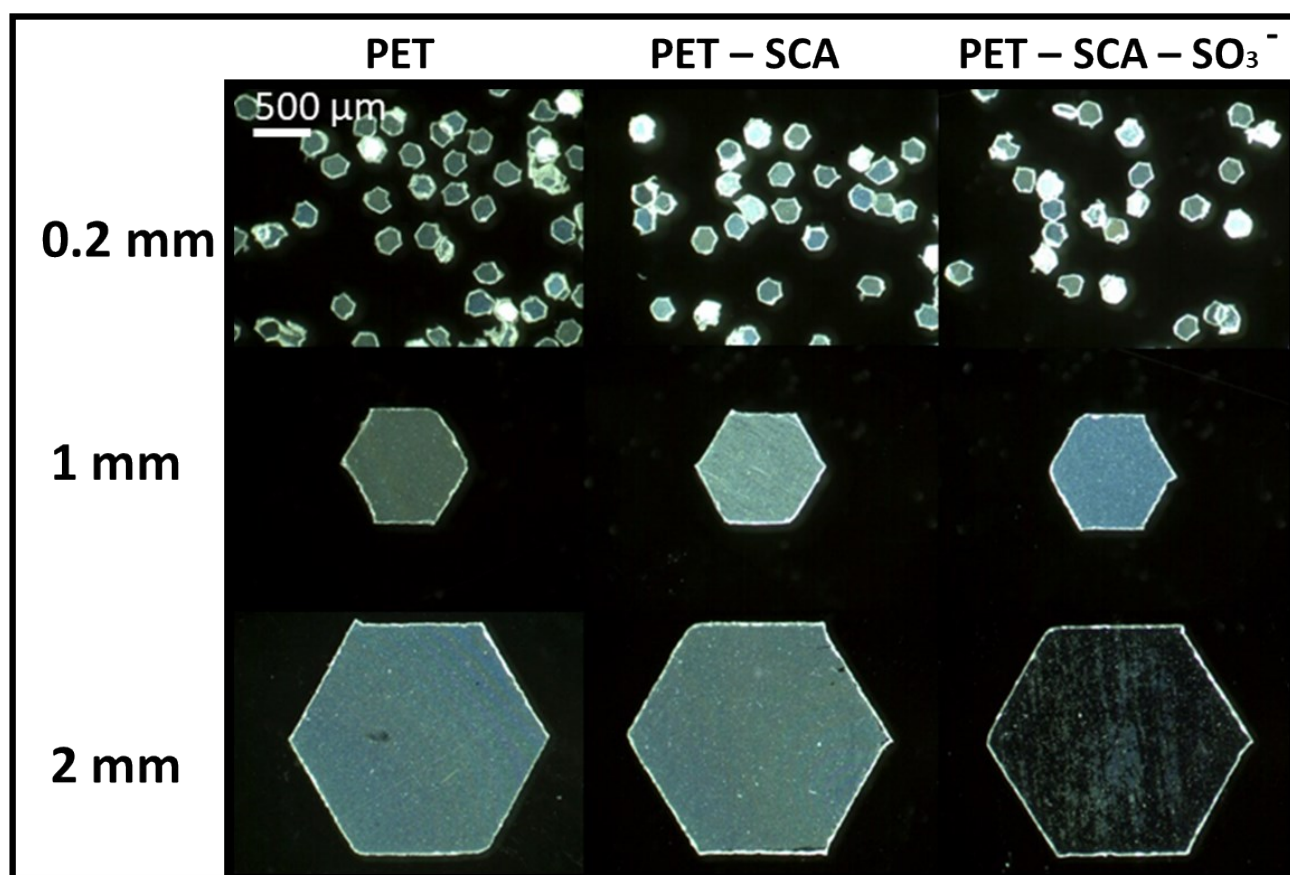


Figure S1. Optical microscopy images of uncoated PET plates.

SEM images used to determine coating thickness of polymer coating

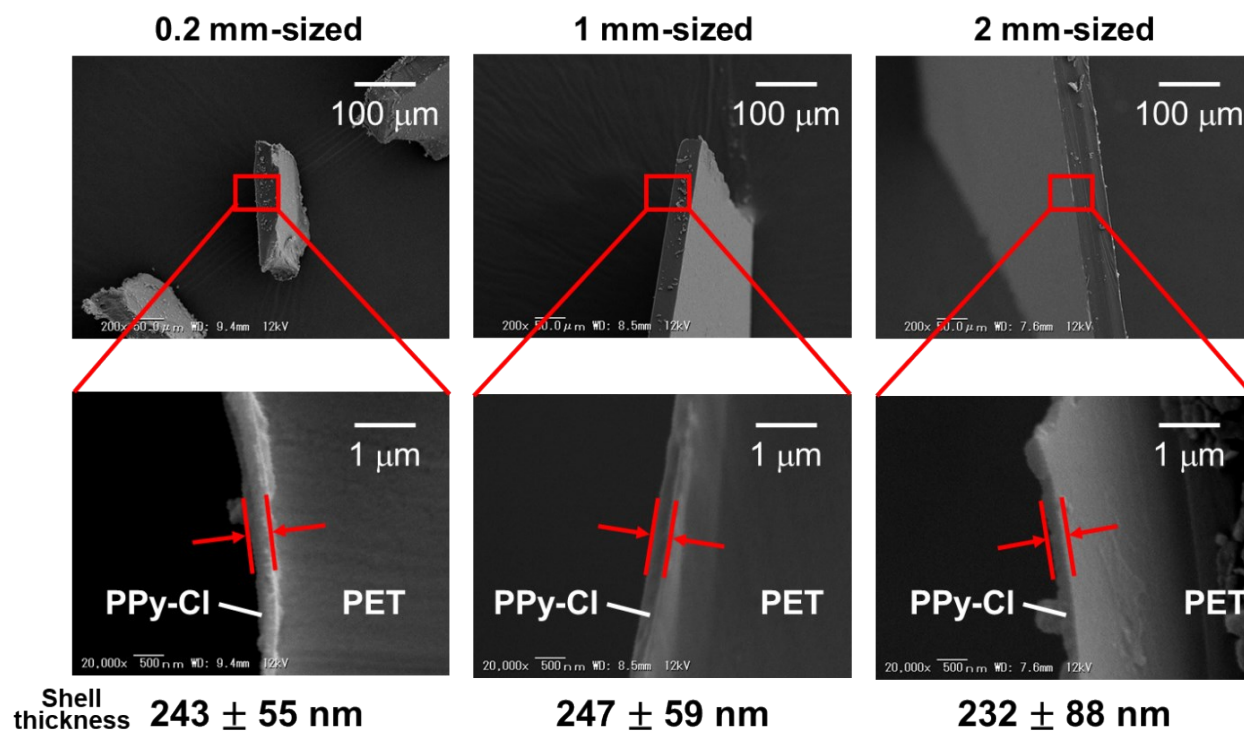
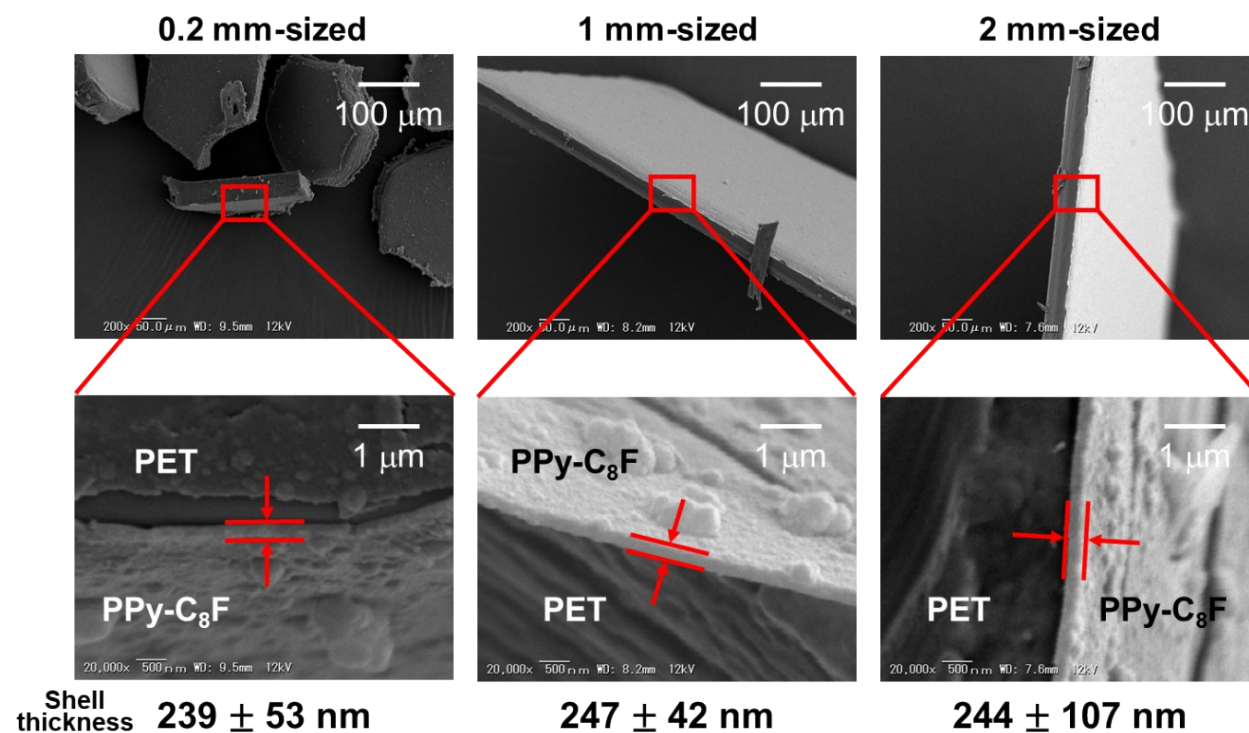


Figure S2. Annotated SEM images of edge coating thickness  $P$  of PPy-Cl on PET substrate.

SEM images used to determine coating thickness of polymer coating



**Figure S3.** Annotated SEM images of edge coating thickness  $P$  of PPy-C<sub>8</sub>F on PET substrate.

**Photos of particle prepared particle bed showing orientation of platelet particles before experiments**

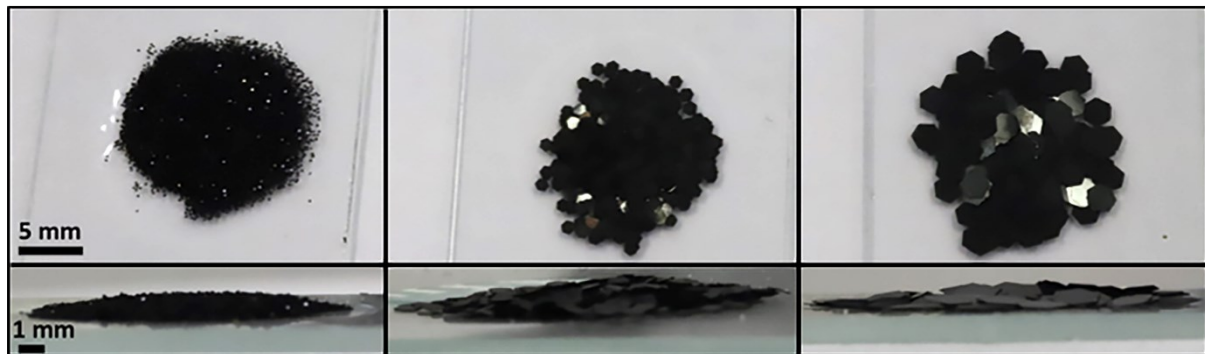


**Figure S4.** Representative particle beds (left to right: 0.2, 1 and 2 mm platelets) after being gently dropped on to metal plate from approximately 5 mm ten times. Top row: top-down image. Bottom row: side image. The photos demonstrate that the bed thickness is less than 2.5 mm in each case

### Mass and volume calculations

Volume and mass % of coating were determined using the thickness of the coating observed in Figures S2 & S3. Particles were treated as if hexagonal prisms in which case volume may be calculated via the following formula:

$$V_{PET\ Plate} = \frac{3\sqrt{3}}{2} S^2 T$$

where  $S$  and  $T$  are the side length and platelet width (Figure S5). The volume of the coating may be determined by treating the edges of the platelet as rectangular prisms of height equal to coating thickness and each face as a hexagonal prism of thickness equal to  $P$  (Figure S2 & S3).

$$V_{Coating} = \left( 2 \times \frac{3\sqrt{3}}{2} S^2 P \right) + (6SP[T + 2P])$$

$$Volume\% = \frac{V_{Coating}}{V_{PET\ Plate}} \times 100\%$$

Similarly,

$$Mass\% = \frac{V_{Coating}\rho_1}{V_{PET\ Plate}\rho_2} \times 100\%$$

Where  $\rho_1$  and  $\rho_2$  are the density of PET and PPy respectively.

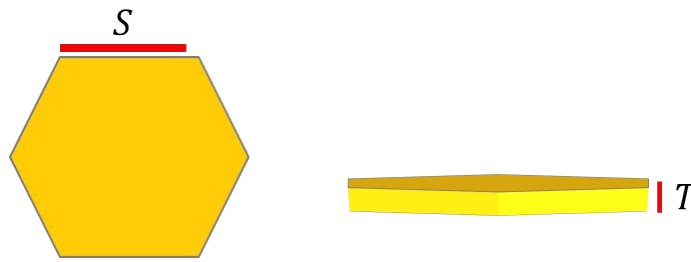


**Figure S5.** Schematic detailing hexagon dimensions

Rolled marbles formed from 0.2 mm platelets before coating with PPy

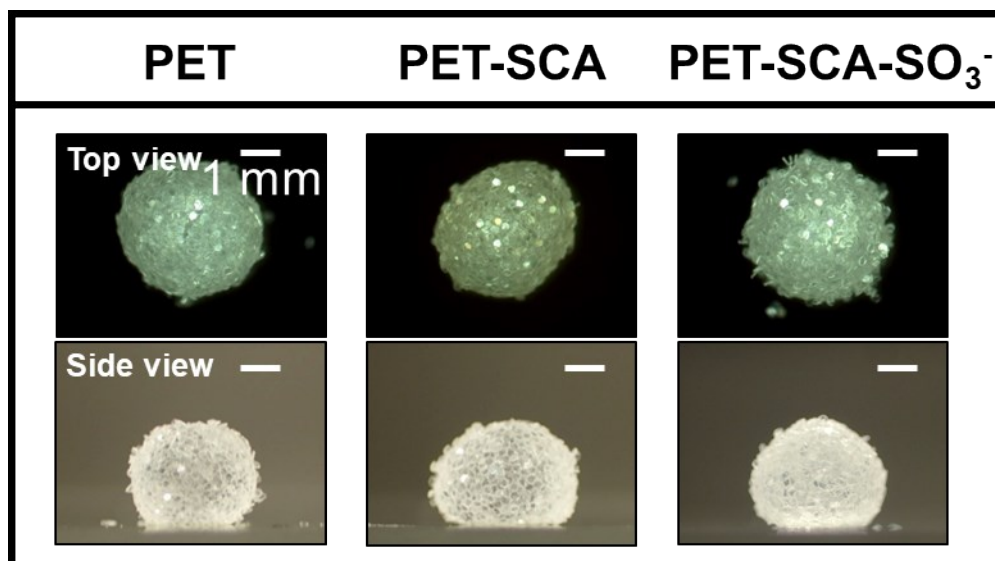
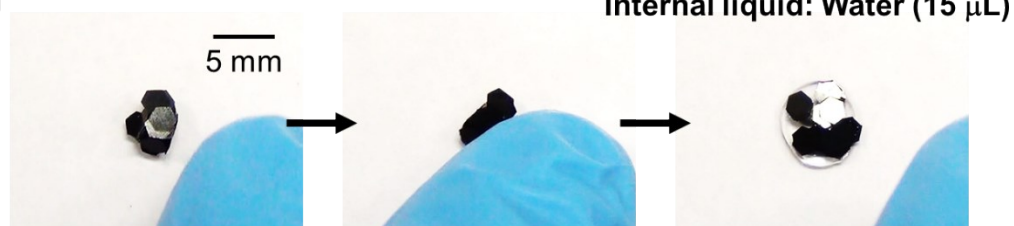


**Figure S6.** Attempts at rolled liquid marbles with 0.2 mm platelets before coating with PPy. Internal liquid is 15  $\mu\text{L}$ . PET plates were unable to maintain stability after compression. The PET-SCA demonstrated some stability due to the lower interfacial energy of the particles after coating. Finally the PET-SCA-SO<sub>3</sub><sup>-</sup> only showed limited stability.

### Rolled liquid marbles being subjected to compressive force

2 mm-sized



1 mm-sized



0.2 mm-sized



**Figure S7.** PET-PPy-Cl stabilised droplets of all tested sizes before and after compressive pressure applied. This demonstrates the tendency of the water to adhere to the platelets due to their hydrophilic nature; this is especially prominent in the 0.2 mm sized plates.



### Rolled liquid marbles being subjected to compressive force

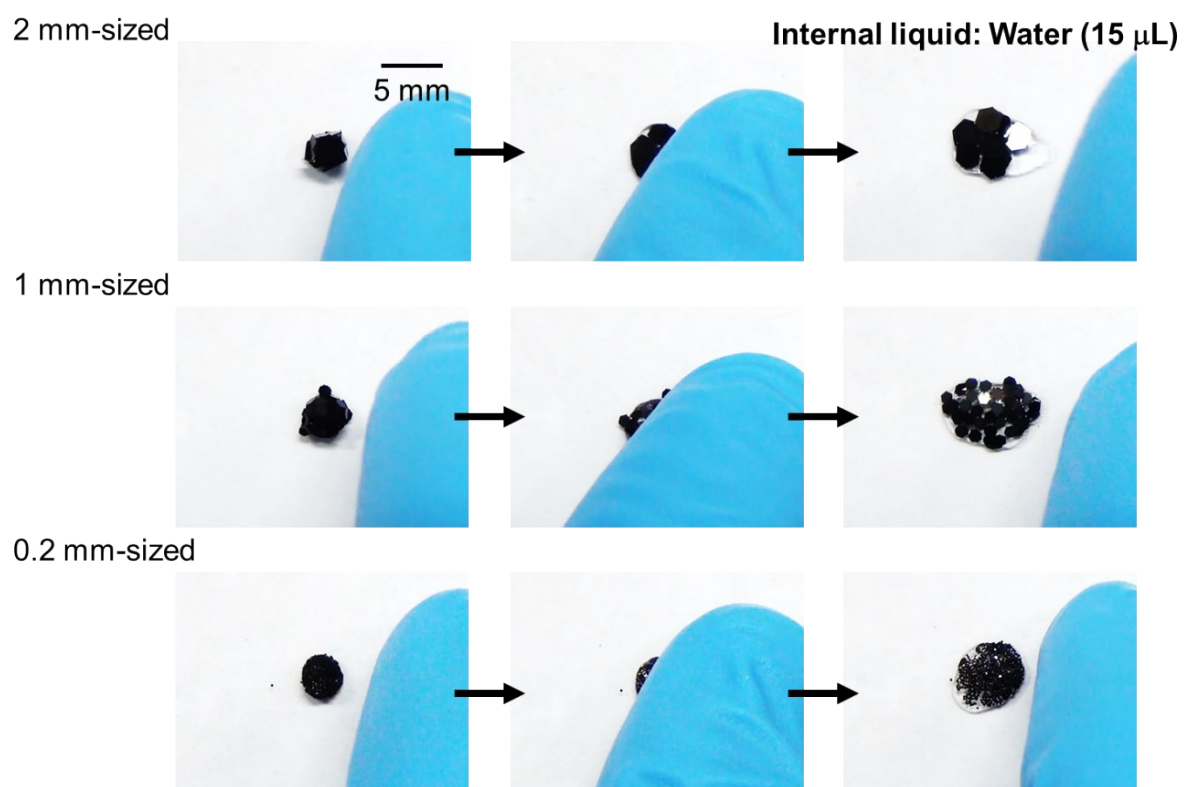


**Figure S8** PET-PPy-C<sub>8</sub>F stabilised droplets of all tested sizes before and after compressive pressure applied. Demonstrating different behaviour of the chemically hydrophobic particles when compared to the hydrophilic Cl<sup>-</sup> doped particles

### Raw & processed electrometer data

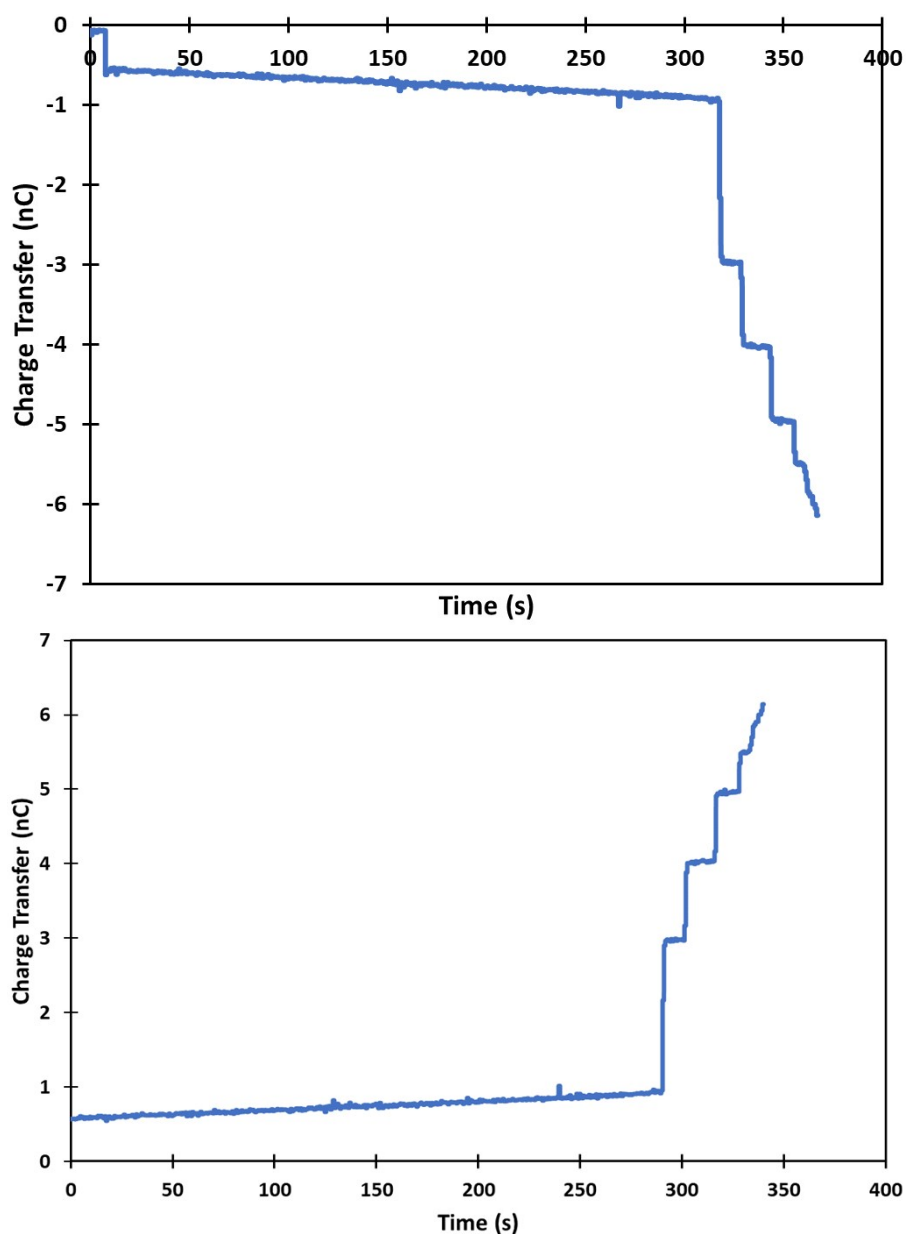


**Figure S9.** Electrometer data collected for 2 mm PET-PPy-C<sub>8</sub>F platelets. Top: Raw data. The initial increase in charge corresponds to the time at which the voltage is applied to the charging plate. Bottom: Data modified to measure magnitude of charge and begin data reporting when the bed begins moving towards the droplet.

## Gravimetric measurements of rolled liquid marbles

**Table S1.** Measured mass percentage of coated polymer plates 15  $\mu\text{L}$  water droplet. Measured by weighing the marble or aggregate before and after evaporation of the internal liquid phase. Used in calculation of number of particles in Figure 3 in manuscript.

| Nominal PET Plate Size (mm) | Mass % PET-PPy-Cl/ $\text{H}_2\text{O}$ in aggregate | Mass % PET-PPy- $\text{C}_8\text{F}$ / $\text{H}_2\text{O}$ in liquid marble |
|-----------------------------|--|--|
| 0.2                         | $42 \pm 11$  | $16 \pm 5$   |
| 1                           | $53 \pm 6$   | $20 \pm 1$   |
| 2                           | $89 \pm 6$   | $9 \pm 1$  |

**Table S2.** Calculated surface area of adsorbed particles based on gravimetric analysis in Table S1.

| Nominal PET Plate Size (mm) | Surface Area of Plate ( $\text{m}^2$ ) | Number of PET-PPy-Cl plates Measured | PET-PPy-Cl Platelet Surface Area ( $\text{m}^2$ ) | Coverage Fraction PET-PPy-Cl plates | Number of PET-PPy- $\text{C}_8\text{F}$ plates Measured | PET-PPy- $\text{C}_8\text{F}$ Platelet Surface Area ( $\text{m}^2$ ) | Coverage Fraction PET-PPy- $\text{C}_8\text{F}$ plates |
|-----------------------------|--|--------------------------------------|---|-------------------------------------|---|--|--|
| 0.2                         | $1.04 \times 10^{-7}$                  | 5693                                 | $5.92 \times 10^{-4}$                             | 10                                  | 629   | $5.47 \times 10^{-5}$  | 1  |
| 1                           | $1.83 \times 10^{-6}$                  | 157                                  | $2.87 \times 10^{-4}$                             | 5                                   | 63  | $1.20 \times 10^{-4}$  | 2  |
| 2                           | $7.77 \times 10^{-6}$                  | 28                                   | $2.18 \times 10^{-4}$                             | 4                                   | 11  | $8.58 \times 10^{-5}$  | 2  |

surface area of a 15  $\mu\text{L}$  droplet is  $2.94 \times 10^{-5} \text{ m}^2$ .

## Determination of theoretical field strength

To determine the force of extraction in Table 3 we must first know  $E$ . For this we use the approach of Morrison.<sup>1</sup> The original work determined the electric field produced by a charged conducting sphere sitting a distance  $h$  above a charge conducting plate at a given applied potential. In our application of this model the conducting sphere is the droplet, the plate is the particle bed and  $h$  represents the drop-bed separation distance. The Morrison model allows determination of the electric vector field components at any point in space close to the droplet. We calculate the total electrostatic field strength as a vector sum of both the radial  $E_r$  and vertical  $E_z$  component of the electric field as close as possible to directly beneath the droplet at a given separation distance

$$E_{Total} = \sqrt{E_r^2 + E_z^2}$$

Consider the data for “1.0 kV” in Figure S9. At a constant potential, as the drop-bed separation distance decreases, the electric field strength increases and so does the extracting force that is acting upon it. Furthermore, as the applied potential increases at a given separation  $h$  so too does the electric field. Conversely, as we decrease potential and/or increase the separation distance the field also decreases. Using this data a value for  $E$  could be determined for drop-bed separation distances experimentally determined from extracted stills at known potentials and used for calculations in Table 3.

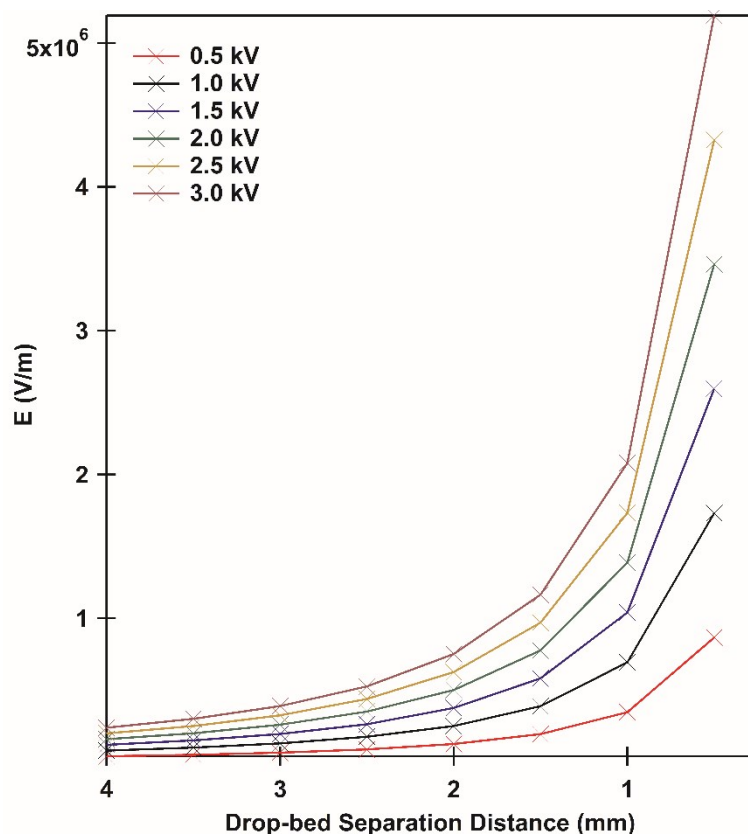


**Figure S10.** Total electrostatic field strength at increasing voltages as a function of decreasing drop-bed separation.

**Table S3.** Calculated electrostatic field values at given separation distanced and applied potentials and measured charge per particle used to determine extraction force on particles in Table 3.

| Voltage (kV) | Drop-bed Separation (mm) | Number of Particles | Charge Before Particle Extraction (nC) | Charge After Particle Extraction (nC) | Charge Per Particle (nC) | E (V/m) $\times 10^5$ | F (mN) |
|--------------|--------------------------|---------------------|--|---------------------------------------|--------------------------|-----------------------|--------|
| 0.5          | 0.560                    | 1                   | 0.80                                   | 4.58                                  | 3.78                     | 7.66                  | 2.89   |
| 1.0          | 1.59                     | 1                   | 1.53                                   | 9.89                                  | 8.36                     | 3.56                  | 2.97   |
| 1.0          | 1.35                     | 1                   | 1.55                                   | 10.4                                  | 8.80                     | 4.53                  | 3.99   |
| 1.0          | 1.29                     | 1                   | 1.55                                   | 8.20                                  | 6.65                     | 4.84                  | 3.22   |
| 1.5          | 2.28                     | 1                   | 2.30                                   | 12.1                                  | 9.80                     | 3.06                  | 3.00   |
| 1.5          | 1.89                     | 1                   | 2.30                                   | 11.1                                  | 8.80                     | 4.10                  | 3.61   |
| 1.5          | 2.10                     | 1                   | 2.45                                   | 17.1                                  | 14.63                    | 3.48                  | 5.08   |
| 2.0          | 2.02                     | 2                   | 3.20                                   | 11.6                                  | 4.20                     | 4.93                  | 2.07   |
| 2.0          | 2.49                     | 2                   | 3.20                                   | 18.2                                  | 7.50                     | 3.53                  | 2.65   |
| 2.0          | 2.78                     | 1                   | 3.18                                   | 15.0                                  | 11.82                    | 2.95                  | 3.48   |
| 2.5          | 3.50                     | 2                   | 4.00                                   | 19.8                                  | 7.90                     | 2.50                  | 1.98   |
| 2.5          | 3.06                     | 2                   | 4.00                                   | 17.3                                  | 6.65                     | 3.14                  | 2.09   |
| 2.5          | 2.98                     | 2                   | 4.60                                   | 27.2                                  | 11.3                     | 3.28                  | 3.70   |
| 3.0          | 5.12                     | 1                   | 4.70                                   | 20.0                                  | 15.3                     | 1.54                  | 2.36   |
| 3.0          | 3.37                     | 3                   | 4.65                                   | 21.0                                  | 5.45                     | 3.20                  | 1.74   |

## References

1. C. A. Morrison, *The potential and electric fields of a conducting sphere in the presence of a charged conducting plane*, Adelphi MD, 1989.